Available online at www.sciencedirect.com
ScienceDirect
Journal of Organometallic Chemistry 693 (2008) 1439–1448
Journal of Organometallic Chemistry
www.elsevier.com/locate/jorganchem

Diphosphine ligand chelation and bridging and regiospecific ortho metalation in the reaction of 4,5-bis(diphenylphosphino)-4-cyclopenten-1,3-dione (bpcd) with $Ir_4(CO)_{12}$: X-ray diffraction structures of $Ir_4(CO)_7(\mu\text{-}CO)_3(bpcd)$, $Ir_4(CO)_5(\mu\text{-}CO)_3(bpcd)(\mu\text{-}bpcd)$, and $HIr_4(CO)_4(\mu\text{-}CO)_3(bpcd)[\mu\text{-}PhP(C_6H_4)C{=}C(PPh_2)C(O)CH_2C(O)]$

William H. Watson [a,*], Guanmin Wu [b], Michael G. Richmond [b,*]

[a] Department of Chemistry, Texas Christian University, Fort Worth, TX 76129, United States
[b] Department of Chemistry, University of North Texas, Denton, TX 76203, United States

Received 23 June 2007; received in revised form 12 July 2007; accepted 13 July 2007
Available online 19 July 2007

Dedicated to the memory of our friend and colleague the late F. Albert Cotton. May Al's contributions never be forgotten and his legacy live on forever.

Abstract

Me_3NO activation of the tetrairidium cluster $Ir_4(CO)_{12}$ (**1**) in presence of the diphosphine ligand 4,5-bis(diphenylphosphino)-4-cyclopenten-1,3-dione (bpcd) furnishes the bpcd-substituted clusters $Ir_4(CO)_{10}(bpcd)$ (**3**) and $Ir_4(CO)_8(bpcd)_2$ (**4**) as the minor and major products, respectively. Cluster **3** has been isolated as the sole observable product from the reaction of $[Ir_4(CO)_{11}Br][Et_4N]$ (**2**) with bpcd in presence of $AgBF_4$ at room temperature. Both **3** and **4** have been isolated and fully characterized in solution by spectroscopic methods. The solid-state structure of **3** reveals that the ancillary bpcd ligand is bound to a single iridium center, with chelating and bridging bpcd ligands found in the X-ray structure of cluster **4**. Cluster **4** is unstable at room temperature and slowly loses CO to afford the hydride-bridged cluster $HIr_4(CO)_4(\mu\text{-}CO)_3(bpcd)[\mu\text{-}PhP(C_6H_4)C{=}C(PPh_2)C(O)CH_2C(O)]$ (**5**). Cluster **5** has been fully characterized in solution by IR and NMR spectroscopies, and the C–H bond activation attendant in the ortho metalation step is shown to occur regioselectively at one of the aryl groups associated with the bridging bpcd ligand. The redox properties of clusters **3**–**5** have been explored and the electrochemical behavior discussed with respect to extended Hückel MO calculations and related diphosphine-substituted cluster compounds prepared by our groups.

Keywords: Iridium clusters; Ligand substitution; Diphosphine ligands; C–H Bond activation; Regioselective ortho metalation

1. Introduction

The ligand substitution chemistry of the tetrametal clusters $M_4(CO)_{12}$ (where M = Co, Rh, Ir) and their phosphine-substituted derivatives has been studied by many different groups over the years with respect to the substitution kinetics and phosphine-ligand distribution about the metal cluster [1]. The reaction between the parent cluster and monodentate phosphines leads to clusters having the general form $M_4(CO)_{12-x}P_x$ (where $x = 1$–4). The major product observed in these reactions is dependent on the concentration and nucleophilicity of the phosphine ligand employed and the method employed to effect activation

* Corresponding authors. Tel.: +1 817 257 7195 (W.H. Watson); tel.: +1 940 565 3548 (M.G. Richmond).
E-mail addresses: w.watson@tcu.edu (W.H. Watson), cobalt@unt.edu (M.G. Richmond).

0022-328X/$ - see front matter © 2007 Elsevier B.V. All rights reserved.
doi:10.1016/j.jorganchem.2007.07.016

of the starting cluster. Thermal, electron-transfer catalysis, reagent promoted oxidative-decarbonylation, and photochemical activation sequences represent the most common methods to facilitate the formal replacement of the CO group by a phosphine ligand. In the case of diphosphine ligands (P–P), the cluster compounds $M_4(CO)_{10}$(P–P) and $M_4(CO)_8$(P–P)$_2$ have been observed as the major products [2–4]. The latter cluster typically accompanies the substitution reaction given the enhanced lability the initially formed $M_4(CO)_{10}$(P–P) cluster.

Recently, we have explored the reactivity of the unsaturated diphosphine 4,5-bis(diphenylphosphino)-4-cyclopenten-1,3-dione (bpcd) with the family of $M_4(CO)_{12}$ tetrametallic clusters (where M = Co, Rh, Ir) and obtained evidence for the sequential substitution of CO and the formation of the corresponding clusters $M_4(CO)_{12-x}(bpcd)_n$ (where $x = 2$, $n = 1$; $x = 4$, $n = 2$). While the Co_4 and Rh_4 clusters have resisted crystallographic characterization, we have been able to structurally characterize the resulting iridium clusters $Ir_4(CO)_{10}$(bpcd) (**3**) and $Ir_4(CO)_8(bpcd)_2$ (**4**) clusters. Cluster **4** exhibits limited stability at room temperature and readily loses CO, followed by ortho metalation of one phenyl groups to furnish the hydride-bridged cluster $HIr_4(CO)_4(\mu\text{-}CO)_3$(bpcd)[$\mu$-PhP($C_6H_4$)C=C($PPh_2$)C(O)$CH_2$C(O)] (**5**). The X-ray structures of clusters **3**–**5** have been determined, and the solid-state structures discussed relative to the corresponding clusters containing the archetypal ligand (*Z*)-$Ph_2PCH{=}CHPPh_2$. The redox properties of clusters **3**–**5** have been examined by electrochemical methods and the data contrasted with the MO results obtained from extended Hückel calculations.

2. Experimental

2.1. General

The parent cluster $Ir_4(CO)_{12}$ (**1**) was prepared from hydrated $IrCl_3$ and CO in EtOH solvent according to the published procedure [5], while [$Ir_4(CO)_{11}Br$][Et_4N] (**2**) was synthesized from **1** and Et_4NBr [6]. The bpcd ligand was synthesized from 4,5-dichloro-4-cyclopenten-1,3-dione and Ph_2PSiMe_3 [7]. All reaction solvents (THF, CH_2Cl_2, 1,2-dichloroethane, and toluene) were distilled from an appropriate drying agent under argon using Schlenk techniques and stored in Schlenk storage vessels with Teflon stopcocks [8]. The IR and NMR solvents were of reagent grade and were degassed with argon prior to their use. The tetra-*n*-butylammonium perchlorate (TBAP) electrolyte employed in the CV studies of clusters **3**–**5** was purchased from Johnson Matthey Electronics and was recrystallized from ethyl acetate/hexane, followed by drying under vacuum for at least 30 h. Combustion analyses on clusters **3** and **5** were performed by Atlantic Microanalysis, Norcross, GA.

The infrared spectrum was recorded on a Nicolet 20 SXB FT-IR spectrometer in a 0.1 mm NaCl cell, using PC control and OMNIC software, while the ^{1}H and ^{31}P NMR spectra were recorded at 200 MHz on a Varian Gemini-200 spectrometer and 121 MHz on a Varian 300-VXR spectrometer. The reported ^{31}P chemical shifts, which were recorded in the proton-decoupled mode, are referenced to external H_3PO_4 (85%), taken to have $\delta = 0$.

2.1.1. Synthesis of $Ir_4(CO)_7(\mu\text{-}CO)_3$(bpcd) (3) and $Ir_4(CO)_5(\mu\text{-}CO)_3$(bpcd)($\mu$-bpcd) (4) from $Ir_4(CO)_{12}$ (1) and bpcd

To a large Schlenk flask was added 0.55 g (0.50 mmol) of $Ir_4(CO)_{12}$ (**1**) and 0.25 g (0.54 mmol) of bpcd, followed by 150 mL of CH_2Cl_2 via cannula. The slurry was cooled to 0 °C and then treated with 90 mg (1.2 mmol) of Me_3NO in one portion. The reaction was allowed to warm to room temperature, with stirring continued overnight. TLC examination the following day revealed the presence of the monosubstituted cluster $Ir_4(CO)_7(\mu\text{-}CO)_3$(bpcd) (**3**), the disubstituted cluster $Ir_4(CO)_5(\mu\text{-}CO)_3$(bpcd)($\mu$-bpcd) (**4**), and unreacted **1**. The solvent was removed under vacuum and the clusters **3** and **4** were sequentially isolated by column chromatography over silica gel using CH_2Cl_2/hexane (3:2) as the mobile phase. The resulting products were recrystallized from a 1:1 mixture of CH_2Cl_2/hexane to afford 0.26 g (35% yield) of cluster **3** and 0.58 g (60% yield based on bpcd consumed) of cluster **4**. Spectroscopic data for **3**: IR (CH_2Cl_2): ν(CO) 2075 (s), 2044 (vs), 2006 (s), 1834 (m), 1796 (m), 1751 (w, sym dione), 1720 (m, antisym dione) cm^{-1}. ^{1}H NMR ($CDCl_3$): δ 7.60–7.20 (m, 20 H, aryl), 3.61 (s, 2 H, CH_2). ^{31}P NMR ($CDCl_3$): δ 6.90 (s). Anal. Calc. for $C_{39}H_{22}Ir_4O_{12}P_2$: C, 30.95; H, 1.47. Found: C, 31.19; H, 1.56%. Spectroscopic data for **4**: IR (CH_2Cl_2): ν(CO) 2069 (w), 2043 (m), 2021 (vs), 1996 (vs), 1962 (s), 1838 (w), 1789 (s), 1766 (m), 1752 (m, sym dione), 1721 (m, antisym, dione) cm^{-1}. ^{1}H NMR ($CDCl_3$): δ 7.75–7.03 (m, 40 H, aryl), 2.93 (AB quartet, 4H, CH_2, $^1J = 21$ Hz). ^{31}P NMR ($CDCl_3$): δ −22.00 (b), −38.60 (s).

2.1.2. Synthesis of $Ir_4(CO)_7(\mu\text{-}CO)_3$(bpcd) (3) from [$Ir_4(CO)_{11}Br$][$Et_4N$] (2) and bpcd

The labile cluster [$Ir_4(CO)_{11}Br$][Et_4N] (**2**) was prepared in situ by refluxing 0.20 g (0.18 mmol) of $Ir_4(CO)_{12}$ and 40 mg (0.19 mmol) of Et_4NBr in 100 mL of THF for 5 h. The solution was concentrated to ca. 20 mL and cluster **2** was then collected by filtration and dried prior to its use in the next step. Cluster **2** was transferred to a Schlenk tube that was then charged with 0.10 g (0.22 mmol) of bpcd, 100 mL of CH_2Cl_2, and 56 mg of $AgBF_4$ and allowed to stir overnight at room temperature. TLC examination confirmed the presence of cluster **3** as the major product, which was isolated by column chromatography and recrystallization as described above. Yield of **3**: 0.15 g (55% based on the amount of cluster **1** employed). No sign of the disubstituted cluster **4** was observed.

2.1.3. Synthesis of $HIr_4(CO)_4(\mu\text{-}CO)_3(bpcd)$ [μ-$PhP(C_6H_4)C{=}C(PPh_2)C(O)CH_2C(O)$] (5) from $Ir_4(CO)_5(\mu\text{-}CO)_3(bpcd)(\mu\text{-}bpcd)$ (4)

To a Schlenk tube was added 0.13 g (0.086 mmol) of cluster **4** and 50 mL of CH_2Cl_2 under argon flush. The vessel was then gently heated at ca. 35 °C overnight and examined by TLC the following day to reveal the complete consumption of cluster **4** and the formation of a new product ($R_f = 0.47$ in CH_2Cl_2) ascribed to the hydrido cluster **5**. Cluster **5** was isolated by column chromatography over silica gel and recrystallized by from CH_2Cl_2/hexane (1:1) to yield cluster **5** in 66% yield (0.11 g). IR (CH_2Cl_2): ν(CO) 2012 (s), 1994 (vs), 1983 (vs), 1859 (w), 1807 (s), 1785 (s), 1749 (m, sym dione), 1718 (s, antisym dione) cm^{-1}. ^1H NMR ($CDCl_3$): δ 7.70–5.95 (m, 39 H, aryl), 3.39 (s, 2 H, CH_2), 2.89 (AB quartet, 2H, CH_2, $^1J = 21$ Hz), −21.00 (m, μ_2-hydride, 1H). ^{31}P NMR ($CDCl_3$): δ 0.93 (d, 1P, $J = 83$ Hz), −4.35 (d, 1P, $J = 102$ Hz), −47.80 (d, 1P, $J = 102$ Hz), −79.79 (d, 1P, $J = 83$ Hz). Anal. Calc. for $C_{65}H_{44}Ir_4O_{11}P_4$: C, 41.19; H, 2.32 . Found: C, 41.48; H, 2.47%.

2.2. X-ray diffraction data for clusters 3–5

Single crystals of the tetrairidium clusters **3**–**5** suitable for X-ray crystallography were grown from a CH_2Cl_2 solution containing each cluster that had been layered with hexane. Unfortunately, only small and poorly formed crystals were found for clusters **4** and **5**, leading to satisfactory but less than ideal refinement. All X-ray data were collected on a Bruker SMART™ 1000 CCD-based diffractometer at room temperature for clusters **3** and **5** and 213 K for cluster **4**. The frames were integrated with the available SAINT software package using a narrow-frame algorithm [9], and the structures were solved and refined using the SHELXTL program package [10]. The molecular structures were checked by using PLATON [11], and all non-hydrogen atoms were refined anisotropically except for the carbon atoms in **5**, which were refined isotropically. All carbon-bound hydrogen atoms were assigned calculated positions and allowed to ride on the attached heavy atom, unless otherwise noted. The presence of a disordered solvent molecule in cluster **5**, which could not be refined by using suitable models, was noted and did not adversely affect the refinement of **5**. The bridging hydride that accompanies the ortho metalation of the phenyl group in cluster **5**, while not be located during refinement, is assumed to be associated with the Ir(3)–Ir(4) (molecule 1) and the Ir(5)–Ir(6) (molecule 2) vectors. Refinement for **3** converged at $R = 0.0329$ and $R_w = 0.0749$ for 3989 independent reflections with $I > 2\sigma(I)$, while refinement for **4** converged at $R = 0.0738$ and $R_w = 0.1848$ for 4859 unique reflections with $I > 2\sigma(I)$. Cluster **5** afforded convergence values of $R = 0.0607$ and $R_w = 0.1039$ for 5989 unique reflections with $I > 2\sigma(I)$ (see Tables 1 and 2).

Table 1
X-ray crystallographic data and processing parameters for the tetrairidium clusters **3**–**5**

Compound	3	4	5
CCDC entry number	606246	606248	606247
Crystal system	Monoclinic	Monoclinic	Triclinic
Space group	$P2_1/c$	$P2_1/n$	$P\bar{1}$
a (Å)	10.670(1)	13.819(5)	11.270(1)
b (Å)	18.197(3)	24.868(8)	20.308(3)
c (Å)	21.154(4)	21.141(7)	31.588(4)
α (°)			99.606(3)
β (°)	96.600(3)	106.959(6)	91.989(3)
γ (°)			93.367(2)
V (Å^3)	4080(1)	6949(4)	7108(2)
Molecular formula	$C_{39}H_{22}Ir_4O_{12}P_2$	$C_{66}H_{44}Ir_4O_{12}P_4$	$C_{65}H_{44}Ir_4O_{11}P_4$ (+disordered solvent)
Formula weight	1513.31	1921.69	1893.68
Formula units per cell (Z)	4	4	4
D_{calc} (Mg/m^3)	2.464	1.837	1.769
λ (Mo Kα) (Å)	0.71073	0.71073	0.71073
Absorption coefficient (mm^{-1})	13.144	7.783	7.606
R_{merge}	0.0957	0.2057	0.1534
Absorption correction	SADABS	SADABS	SADABS
Abs correction factor	0.8345/0.1753	0.6246/0.2712	0.7962/0.3842
Total reflections	23136	43732	36300
Independent reflections	5342	10907	15271
Data/restraint/parameters	5342/0/505	10907/0/445	15271/0/932
R	0.0329	0.0738	0.0607
R_w	0.0749	0.1848	0.1039
Goodness-of-fit on F^2	0.958	0.905	0.779
$\Delta\rho$(maximum), $\Delta\rho$(minimum) (e/Å^3)	1.952, −1.811	4.111, −2.056	1.545, −1.024

2.3. Electrochemical data

All cyclic and differential pulse voltammograms were recorded on a PAR Model 273 potentiostat/galvanostat, equipped with positive feedback circuitry to compensate for *i*R drop. An airtight, three-electrode design CV cell was used, with a platinum disk (1.0 mm diameter) serving as the working and auxiliary electrodes. The reference electrode utilized a silver wire as a quasi-reference electrode, and the reported potential data were referenced to the formal potential of the Cp_2Fe/Cp_2Fe^+ (internally added) redox couple, taken to have $E_{1/2} = 0.307$ V [12].

2.4. Extended Hückel MO calculations

The extended Hückel calculations on clusters **3** and **4** were carried out using the original program developed by Hoffmann [13], as modified by Mealli and Proserpio [14].

Table 2
Selected bond distances (Å) and angles (°) in the tetrairidium clusters **3**–**5**

$Ir_4(CO)_7(\mu\text{-}CO)_3$(bpcd) (**3**)			
Bond distances (Å)			
Ir(1)–Ir(4)	2.7452(7)	Ir(1)–Ir(3)	2.7545(6)
Ir(1)–Ir(2)	2.7855(6)	Ir(2)–Ir(3)	2.7022(7)
Ir(2)–Ir(4)	2.7126(7)	Ir(3)–Ir(4)	2.7165(7)
Ir(1)–P(1)	2.314(3)	Ir(1)–P(2)	2.284(3)
P(1)···P(2)	3.171(9)		
Bond angles (°)			
C(30)–Ir(1)–P(2)	98.7(3)	C(31)–Ir(1)–P(2)	90.0(3)
C(30)–Ir(1)–P(1)	103.4(3)	C(31)–Ir(1)–P(1)	91.5(3)
P(2)–Ir(1)–P(1)	87.20(9)	Ir(1)–C(31)–Ir(2)	82.0(4)
Ir(1)–C(30)–Ir(4)	77.5(4)	Ir(4)–C(34)–Ir(2)	80.8(5)
$Ir_4(CO)_5(\mu\text{-}CO)_3(bpcd)_2$ (**4**)			
Bond distances (Å)			
Ir(1)–Ir(2)	2.713(2)	Ir(1)–Ir(4)	2.735(2)
Ir(1)–Ir(3)	2.745(2)	Ir(2)–Ir(4)	2.720(2)
Ir(2)–Ir(3)	2.738(2)	Ir(3)–Ir(4)	2.770(2)
Ir(1)–P(2)	2.284(7)	Ir(2)–P(1)	2.313(7)
Ir(3)–P(3)	2.283(7)	Ir(3)–P(4)	2.284(7)
P(1)···P(2)	3.72(1)	P(3)···P(4)	3.14(1)
Bond angles (°)			
C(59)–Ir(1)–P(2)	92.4(7)	C(60)–Ir(1)–P(2)	104.1(8)
P(3)–Ir(3)–P(4)	87.0(3)	C(1)–P(1)–Ir(2)	122.2(9)
C(2)–P(2)–Ir(1)	115.0(9)	C(31)–P(3)–Ir(3)	105.3(9)
C(30)–P(4)–Ir(3)	104.7(8)	C(2)–C(1)–P(1)	130(2)
C(1)–C(2)–P(2)	130(2)	C(31)–C(30)–P(4)	123(2)
C(30)–C(31)–P(3)	117(2)	Ir(3)–C(60)–Ir(1)	81(1)
Ir(3)–C(61)–Ir(4)	83(1)		
$HIr_4(CO)_4(\mu\text{-}CO)_3$(bpcd)[$\mu$-PhP($C_6H_4$)C=C($PPh_2$)C(O)$CH_2$C(O)] (**5**)			
Bond distances (Å)			
Molecule 1		Molecule 2	
Ir(1)–Ir(3)	2.670(2)	Ir(5)–Ir(8)	2.674(2)
Ir(1)–Ir(2)	2.699(2)	Ir(5)–Ir(7)	2.753(2)
Ir(1)–Ir(4)	2.764(2)	Ir(5)–Ir(6)	2.925(2)
Ir(2)–Ir(3)	2.744(2)	Ir(6)–Ir(8)	2.751(2)
Ir(2)–Ir(4)	2.763(2)	Ir(6)–Ir(7)	2.766(2)
Ir(3)–Ir(4)	2.914(2)	Ir(7)–Ir(8)	2.705(2)
Ir(1)–P(4)	2.288(8)	Ir(6)–P(5)	2.294(8)
Ir(2)–P(3)	2.319(8)	Ir(6)–P(6)	2.312(8)
Ir(4)–P(1)	2.314(8)	Ir(7)–P(7)	2.331(8)
Ir(4)–P(2)	2.324(8)	Ir(8)–P(8)	2.281(8)
Ir(3)–C(55)	1.95(4)	Ir(5)–C(120)	2.12(3)
P(1)···P(2)	3.18(1)	P(5)···P(6)	3.19(1)
P(3)···P(4)	3.65(1)	P(7)···P(8)	3.68(1)
Bond angles (°)			
Molecule 1		Molecule 2	
P(1)–Ir(4)–P(2)	86.7(3)	P(5)–Ir(6)–P(6)	87.8(3)
C(8)–P(1)–Ir(4)	107(1)	C(73)–P(5)–Ir(6)	104.7(9)
C(12)–P(2)–Ir(4)	103(1)	C(77)–P(6)–Ir(6)	105.7(9)
C(37)–P(3)–Ir(2)	118(1)	C(102)–P(7)–Ir(7)	114.1(9)
C(38)–P(4)–Ir(1)	112.9(9)	C(106)–P(8)–Ir(8)	115.8(9)
C(55)–Ir(3)–C(6)	93(1)	C(120)–Ir(5)–C(70)	88(1)
C(55)–Ir(3)–C(2)	88(1)	C(120)–Ir(5)–C(67)	92(1)

The weighted H_{ij}s contained in the program were employed in the calculations. The input Z-matrix for model compounds $Ir_4(CO)_7(\mu\text{-}CO)_3$(bpcd-$H_4$) (**3**-$H_4$) and $Ir_4(CO)_5(\mu\text{-}CO)_3$(bpcd-$H_4$)($\mu$-bpcd-$H_4$) (**4**-$H_8$) were constructed using the X-ray data of clusters **3** and **4** with the phenyl groups belonging to the ligand(s) replaced by hydrogen atoms. Here the P–H bond distances were set at 1.41 Å [15].

3. Results and discussion

3.1. Synthesis, spectroscopic data, and molecular structures of 3 and 4

The reaction between $Ir_4(CO)_{12}$ (**1**) and a slight excess of bpcd was examined under controlled thermolysis in CH_2Cl_2, 1,2-dichloroethane, and toluene solvents, with the substituted clusters $Ir_4(CO)_{10}$(bpcd) (**3**) and $Ir_4(CO)_8$(bpcd)$_2$ (**4**) found as the minor and major products, respectively, in addition to unreacted **1** and trace amounts of cluster **5** (vide infra). The amount of the latter cluster, which derives from cluster **4**, can be minimized by monitoring the thermolysis reaction by TLC analysis and terminating the reaction upon the consumption of the bpcd ligand. Treatment of a mixture containing **1** and bpcd (slight excess) with Me_3NO (2 equiv. relative to **1**) qualitatively gave the same product distribution of clusters **3** and **4** as found in the thermolysis reactions. No attempts were made to optimize the yield of cluster **3** in these reactions as mixtures of **3** and **4** were always obtained, paralleling the reported reactivity of cluster **1** with the unsaturated diphosphine ligand (*Z*)-$Ph_2PCH{=}CHPPh_2$ [4b,4c]. Cluster **3** could be isolated as the sole product from the reaction of the halide-substituted cluster [$Ir_4(CO)_{11}Br$][Et_4N] (**2**) with added bpcd in the presence of $AgBF_4$. Here the silver-promoted abstraction of the bromide ligand from cluster **2** generates the unsaturated cluster "$Ir_4(CO)_{11}$", whose reaction with bpcd gives cluster **3** free from cluster **4**. This particular protocol has been effectively demonstrated by numerous research groups and allows the degree of ligand substitution in this genre of cluster to be carefully controlled [4c–e,16]. Scheme 1 outlines the reactions leading to clusters **3** and **4** starting from **1** [17]. Both product clusters were conveniently isolated by column chromatography over silica gel as mildly air-sensitive solids. While clusters **3** and **4** may be handled for short periods of time as solids in the atmosphere, solutions containing these clusters appear to be more oxygen sensitive, exhibiting noticeable decomposition upon exposure to oxygen after only a few hours. Cluster **4** was also found to be thermally sensitive and is best stored under CO (vide infra).

Both **3** and **4** were characterized in solution by IR and NMR spectroscopies. Terminal carbonyl stretching bands were observed at 2075 (s), 2044 (vs), and 2006 (s) cm^{-1} for cluster **3** in CH_2Cl_2, along with two moderately intense bridging ν(CO) bands at 1834 and 1796 cm^{-1}, whose collective frequencies are in close agreement with those IR data reported for $Ir_4(CO)_{10}$[(*Z*)-$Ph_2PCH{=}CHPPh_2$] and related Ir_4 clusters possessing an ancillary diphosphine ligand [4c–e]. The IR spectrum also displays two lower energy ν(CO) bands at 1751 (w) and 1720 cm^{-1} that are readily assigned to the vibrationally coupled carbonyl groups associated with the dione moiety [18]. The ^{1}H NMR spectrum of **3**

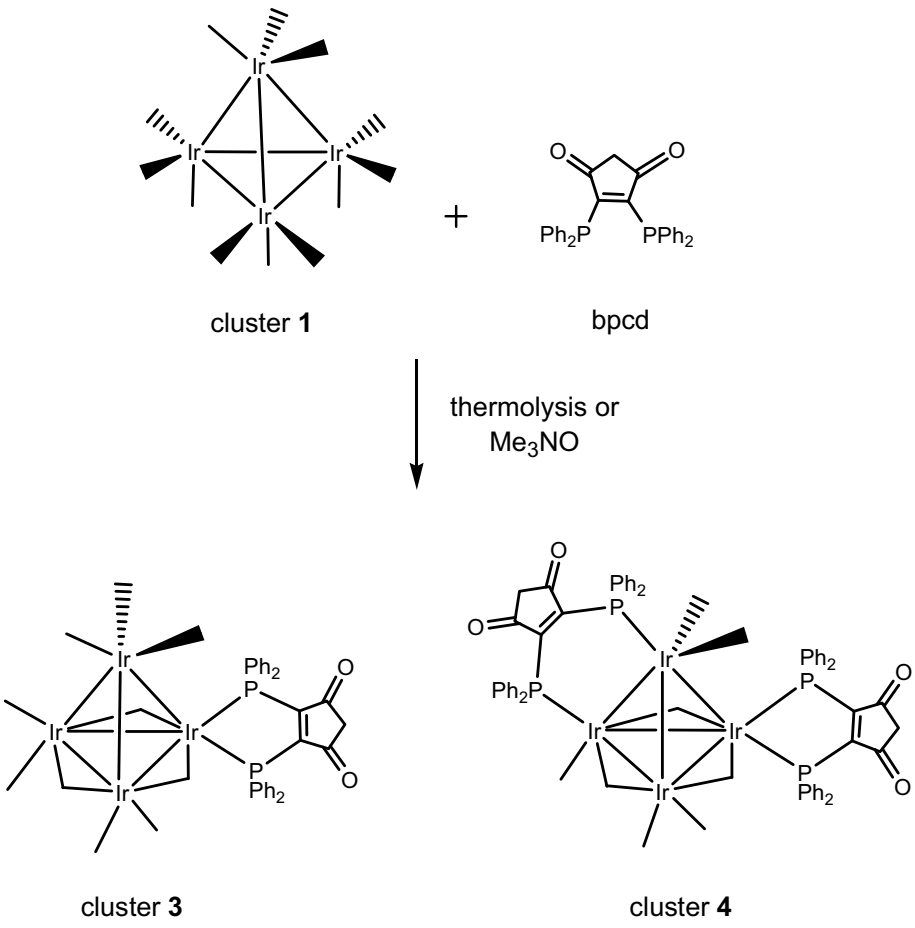

Scheme 1.

recorded in $CDCl_3$ reveals a multiplet for the aromatic hydrogens at δ 7.60–7.20 and singlet at δ 3.61 for the methylene group of the dione ring. The ^{31}P NMR spectrum revealed the presence of single phosphorus resonance at δ 6.90 that supports the presence of a chelating bpcd ligand in **3**. The thermal ellipsoid plot of **3** is depicted in Fig. 1, where the bpcd ligand is shown to function as a chelating ligand through coordination to the Ir(1) center. Cluster **3** consists of an Ir_4 tetrahedral core in accordance with its 60-valence electron count. The Ir–Ir bond lengths range from 2.7022(7) Å [Ir(2)–Ir(3)] to 2.7855(6) Å [Ir(1)–Ir(2)] and display a mean length of 2.7361 Å in agreement with those Ir–Ir bond distances found in related clusters [19]. The bpcd ligand is bound to one of the three basal iridium atoms in a manner similar to the ligand-chelated clusters $Ir_4(CO)_7(\mu\text{-}CO)_3$(dppbz) and $Ir_4(CO)_7(\mu\text{-}CO)_3$[1,2-$Me_2$As-($C_6H_4$)] [4i,20], with the P(1) and P(2) moieties exhibiting axial and equatorial dispositions, respectively. The basal plane that is defined by the Ir(1)–Ir(2)–Ir(4) atoms in **3** displays three edge-bridging carbonyl groups, as is common with this genre of Ir_4 cluster. The Ir(1)–P(1) and Ir(2)–P(2) distances of 2.314(3) Å and 2.284(3) Å, respectively, and the P(1)–Ir(1)–P(2) bond angle of 87.20(9)° are in agreement with those distances and angles found by us in other cluster compounds possessing a chelating bpcd ligand [21]. The remaining bond distances and angles are unremarkable.

The IR spectrum of **4** revealed ν(CO) bands at 2069 (w), 2043 (m), 2021 (vs), 1996 (vs), 1962 (s), 1838 (w), 1789 (s), and 1766 (m) cm^{-1}, of which the latter three ν(CO) bands belong to semi-bridging and bridging carbonyl groups. The overall shift in the frequency of the carbonyl groups in **4** relative to those in cluster **3** is consistent with the presence of two bpcd ligands in the coordination sphere of cluster **4**. Insufficient spectral resolution between the bridging and chelating bpcd ligands in **4** gives rise to broad ν(CO) bands at 1752 (m) and 1721 (m) cm^{-1} for the two dione moieties. The ^1H NMR spectrum exhibits a multiplet at δ 7.75–7.03 for the aromatic hydrogens and an AB quartet at δ 2.93 for both bpcd ligands, while the ^{31}P NMR spectrum displays one broad resonance at δ −22.00 and a sharp resonance at δ −38.60. The NMR data cannot be reconciled with the solid-state structure of **4** and suggest that the ancillary CO groups are fluxional at room temperature. Dynamic CO scrambling in the diphosphine-substituted clusters $Ir_4(CO)_{10}$(P–P) and $Ir_4(CO)_8$[(*Z*)-$Ph_2PCH{=}CHPPh_2$]$_2$ is a phenomenon that is well documented, precluding the observation of the limiting ^1H and ^{31}P NMR spectra of these clusters at room temperature.

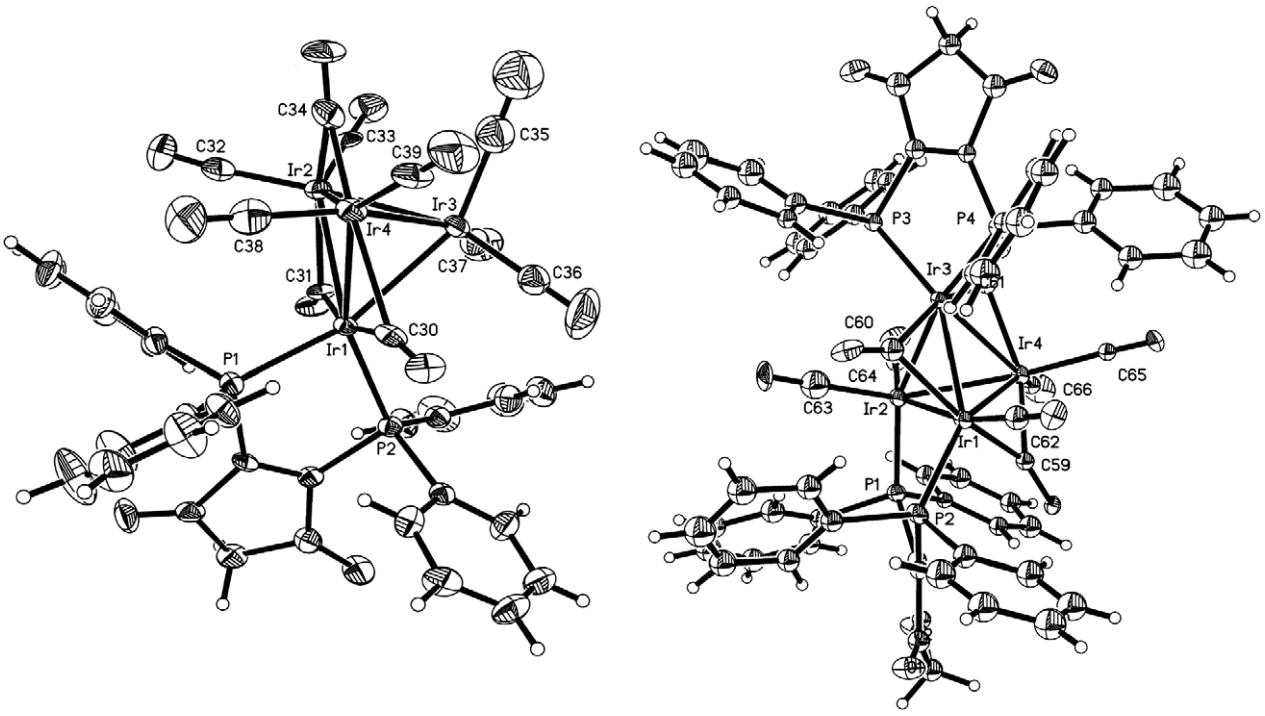

Fig. 1. Thermal ellipsoid plots of $Ir_4(CO)_7(\mu\text{-}CO)_3(bpcd)$ (**3**, left) and $Ir_4(CO)_5(\mu\text{-}CO)_3(bpcd)_2$ (**4**, right) showing the thermal ellipsoids at the 50% probability level.

The solid-state structure of **4** is depicted in Fig. 1, where a tetrahedral core of iridium atoms that exhibits both bridging and chelating bpcd ligands is confirmed. A check of the recent Cambridge Structural Database confirms **4** as the first Ir_4 cluster to possess intact chelating and bridging diphosphine ligands. Other than **4**, all structurally characterized $Ir_4(CO)_8(P\text{–}P)_2$ clusters, to date, contain two bridging diphosphine ligands. Cluster **4** is electron precise and contains 60 valence electrons. The bridging bpcd ligand spans the Ir(1)–Ir(2) vector and the chelating bpcd ligand is bound by the Ir(3) center. The Ir–Ir bond distances range from 2.713(2) Å [Ir(1)–Ir(2)] to 2.770(2) Å [Ir(3)–Ir(4)] with a mean length of 2.737 Å. The Ir(1)–Ir(3)–Ir(4) atoms give rise to a basal triangle that includes three edge-bridging CO groups. These μ_2-CO groups are asymmetrically bound to the three basal Ir–Ir bonds based on distances that range from 2.02(3) Å [Ir(3)–C(61)] to 2.18(3) Å [Ir(1)–C(60)] and exhibit an average distance of 2.10 Å. The elongation of the Ir(3)–Ir(4) vector relative to the other five iridium-iridium bond distances is presumed to derive from a steric perturbation imposed on the metal core by the bpcd that is chelated to the Ir(3) center. Similar diphosphine-induced metal–metal bond elongations have been observed in other structurally characterized clusters from our groups [22]. The presence of different bpcd ligands in **4** facilitates a ground-state structural comparison of the two ligands as a function of their coordination mode. The bridging of the Ir(1) and Ir(2) atoms by the P(2) and P(1) moieties, respectively, is accompanied by a substantial structural perturbation within the ligand frame due to a ''stretching'' of phosphines across the Ir(1)–Ir(2) vector. Here the internuclear P(1)···P(2) distance of 3.72(1) Å is 0.58 Å larger than the analogous P(3)···P(4) distance [3.14(1) Å] in the chelating bpcd ligand in **4** and the internuclear P···P distance in other bpcd-chelated clusters structurally characterized by us [21]. Unfavorable binding of the bpcd ligand across the Ir(1)–Ir(2) vector manifests itself in significant deviation in the bond angles associated with the C(1)–P(1)–Ir(2) [122.2(9)°] and C(2)–P(2)–Ir(1) [115.0(9)°] linkages with respect to the anticipated bond angle of 109° expected for a tetracoordinate phosphorus atom. The bond angles of 105.3(9)° and 104.7(8)° found for the related C(31)–P(3)–Ir(3) and C(30)–P(4)–Ir(3) linkages in the chelated-bpcd ligand provide a convenient basis for an internal comparison of this structural perturbation as a function of the ligand coordination mode. These latter two bond angles support the notion that a chelating bpcd ligand is thermodynamically more stable than its bridging counterpart in third-row metal clusters, as has been demonstrated by us for the isomerization of diphosphine ligands in the triosmium clusters $Os_3(CO)_{10}(P\text{–}P)$ (where P–P = various diphosphine ligands) [23].

3.2. Synthesis, spectroscopic data, and molecular structure of *5*

The observation of minor amounts of cluster **5** in our initial thermolysis reactions of $Ir_4(CO)_{12}$ with bpcd supported the involvement of cluster **4**, with its two bpcd ligands, as the direct precursor to **5**. This fact was subsequently

confirmed by control experiments employing cluster **4**; gently heating samples of **4** in CH_2Cl_2 furnished cluster **5** as the sole observed product based on TLC and ^{31}P NMR spectroscopy. Eq. (1) illustrates this particular reaction. The rate for the conversion of **4** → **5** at 50 °C in 1,2-dichloroethane solvent has been determined by following the optical changes of the 650 nm band of cluster **4** using UV–Vis spectroscopy. The measured first-order rate constant of $1.18(5)\times10^{-4}\,s^{-1}$ ($t_{1/2}\approx 2$ h) is consistent with the general lability of cluster **4** in the absence of CO and suggests a rate-limiting step involving a dissociative loss of CO or an associative interchange process where a π bond from one of the aryl groups serves to displace a CO ligand. Of these two possible processes, we favor the former one since the conversion to **5** is retarded in the presence of CO (1 atm) [24]. Cluster **5** could be isolated from preparative thermolysis reactions employing **4** via chromatographic separation, followed by recrystallization, in good yields as a slightly air-sensitive green solid.

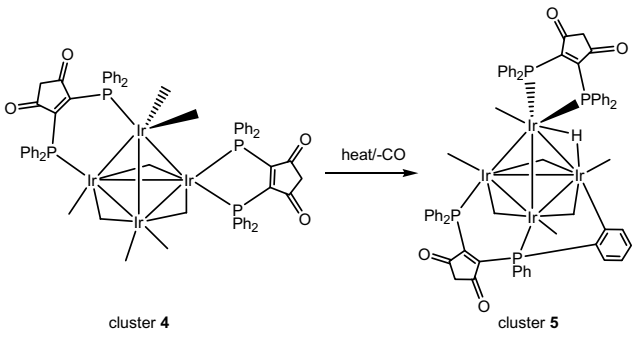

(1)

The ^1H NMR spectrum of **5** recorded in $CDCl_3$ revealed a singlet at δ 3.39 and an AB quartet centered at δ 2.89 for the methylene groups belonging to the two bpcd ligands, along with a high-field hydride at δ −21.00 consistent with an ortho metalation of one of the ancillary aryl rings and the formulated structure for cluster **5**. The observation of four ^{31}P resonances in the ^{31}P NMR spectrum of **5** reveals that the phosphine moieties associated with the two bpcd ligands are statically bound and occupy distinct environments about the Ir_4 frame. That these phosphine ligands are not subject to a fluxional equilibration was corroborated by ^{31}P NMR EXSY measurements. Fig. 2 shows the thermal ellipsoid plot of one of the two crystallographically independent molecules of **5** found in the unit cell. Apart from some minor differences between related bond distances and angles, both molecules of **5** are structurally identical. The presence of bridging and chelating bpcd ligands and, more importantly, the loss of CO from cluster **4** and the regiospecific ortho metalation of an aryl group from the bridging bpcd ligand are established. The Ir–Ir bond distances range from 2.670(2) Å [Ir(1)–Ir(3)] to 2.914(2) Å [Ir(3)–Ir(4)] and exhibit a mean distance of 2.759 Å. While the hydride ligand was not directly located in the difference maps during refinement, it has been assigned to the Ir(3)–Ir(4) vector in keeping with

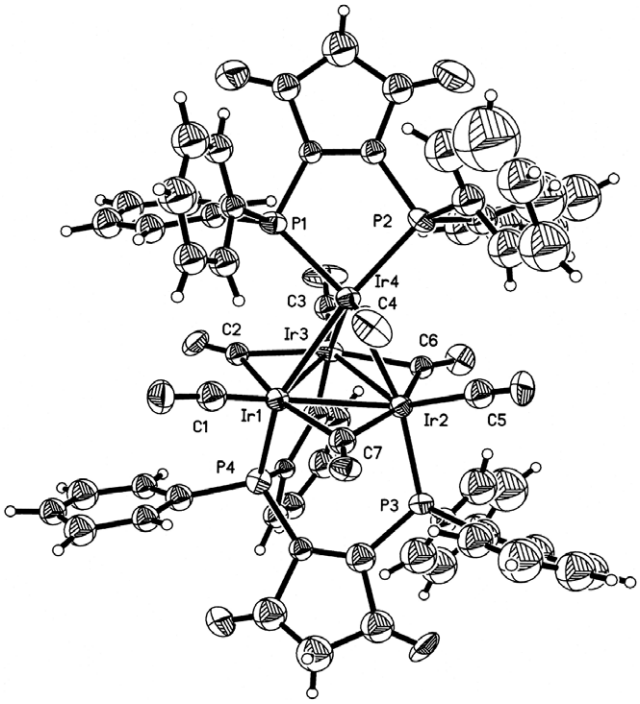

Fig. 2. Thermal ellipsoid plot of one of the two independent molecules of $HIr_4(CO)_4(\mu\text{-}CO)_3(bpcd)[\mu\text{-}PhP(C_6H_4)C{=}C(PPh_2)C(O)CH_2C(O)]$ (**5**) showing the thermal ellipsoids at the 50% probability level.

metal–metal bond distance trends found in other hydride-bridged metal clusters [25]. The ortho metalation of one of the aryl groups from the bridging bpcd ligand is verified by the Ir(3)–C(55) vector, whose bond length of 1.95(3) Å is in good agreement with those Ir–C bond distances found in other polynuclear iridium clusters containing an ortho-metalated aryl group [26]. The general molecular structure and the capping of the axial face of the basal triangle that is defined by the Ir(1)–Ir(2)–Ir(3) atoms by the five-electron donor ligand $\mu\text{-}[Ph_2PC{=}C\{PPh(C_6H_4)\}C(O)CH_2C(O)]$ are identical to hydride-bridged cluster $HIr_4(CO)_7[(Z)\text{-}Ph_2CH{=}CHPPh_2][\mu\text{-}(Z)\text{-}Ph_2PCH{=}CH\{PPh(C_6H_4)\}]$ reported by Albano et al. [4b] and Ros et al. [4c]. The remaining bond distances and angles are unremarkable and require no comment.

3.3. Electrochemical and molecular orbital properties of clusters 3–5

The redox properties of clusters **3**–**5** were investigated by a combination of cyclic and differential pulse voltammetries due to the presence of the ancillary bpcd ligand(s). This particular diphosphine ligand and related diphosphine analogs have the ability to serve as well-defined electron reservoirs due to the presence of a low-lying π^* orbital that is localized over the central carbocyclic platform of the diphosphine ligand. All voltammetric data were collected at a platinum disk electrode (area 0.0079 cm^2) in CH_2Cl_2 containing 0.2 M TBAP as the supporting electrolyte. Cyclic voltammetric investigation of cluster **3** at a scan rate of

0.25 V/s over the potential range of 1.0 V to −1.0 V revealed the presence of a reversible one-electron reduction at $E_{1/2} = -0.61$ V [27]. The observation of single reduction wave for $0/1^-$ redox couple and its recorded potential are consistent with the electrochemical behavior found by us in other metal clusters containing a bpcd ligand [21]. The site of electron accession and the nature of the LUMO in **3** were addressed by carrying out extended Hückel MO calculations on the model cluster $Ir_4(CO)_7(\mu\text{-}CO)_3(bpcd\text{-}H_4)$ (**3**-H_4). Here the phenyl groups were replaced by hydrogens in order to simplify the calculations. The LUMO, which occurs at an energy of −10.43 eV, is localized exclusively on the dione ring and exhibits π^* character that is readily traced to the ψ_4 MO of the related 6π-electron systems maleic anhydride and hexatriene [28]. The experimentally measured reduction potential for the $0/1^-$ redox wave, calculated energy, and parentage of the LUMO in **3** are unexceptional with respect to those data reported by us in the related clusters $Ru_3(CO)_{10}(bpcd)$, $PhCCo_3(CO)_2(bpcd)\text{-}Cp_2$, and $FeCo_2(\mu_3\text{-}S)(CO)_7(bpcd)$, all of which contain a chelating bpcd [21a,21b,21d,29].

The presence of two bpcd ligands in cluster **4** raises the interesting possibility of a site-selective reduction that is dependent on the coordination mode of the ancillary diphosphine ligand. Alternatively, extensive electron delocalization between the π^* repositories of these ligands could furnish a mixed-valence compound with the Ir_4 link modulating the electron migration between the two reduction sites. The CV of **4** recorded at room temperature exhibits two reversible one-electron reductions at $E_{1/2} = -0.68$ and −0.87 V, corresponding to successive $0/1^-$ reductions at the bridging and chelating bpcd ligands, respectively (vide infra). The differential pulse voltammogram of **4** recorded under analogous conditions is depicted in Fig. 3, where the proposed one-electron stoichiometry associated with these reductions is readily verified. The calculated comproportionation constant (K_c) was determined to on the order 1600, confirming only weak mixed-valence character and minimal electron delocalization between the two bpcd π^* sites in cluster **4**.

The orbital composition of the LUMO and LUMO + 1 that serve as the sequential reduction sites in cluster **4** was determined by carrying out extended Hückel MO calculations. Here calculations on the model cluster $Ir_4(CO)_5(\mu\text{-}CO)_3(bpcd\text{-}H_4)(\mu\text{-}bpcd\text{-}H_4)$ (**4**-H_8) revealed two closely lying empty orbitals at −10.43 eV and −10.18 eV having π^* parentage derived from the bridging and chelating bpcd ligands, respectively, as shown below. The orbital composition of the LUMO and LUMO + 1 in **4** is similar to that found in the vast majority of bpcd and bma compounds reported and mimics that of ψ_4 found in the 6π-electron systems maleic anhydride and hexatriene. In the case of the model cluster $Ir_4(CO)_5(\mu\text{-}CO)_3(bpcd\text{-}H_4)(\mu\text{-}bpcd\text{-}H_4)$ (**4**-H_8), these data indicate that the first reduction step is site selective and occurs at the bridging bpcd ligand. This is interesting because the triruthenium cluster $Ru_3(CO)_5\text{-}(\mu_3\text{-}CO)(\mu_3\text{-}NPh)(bpcd)_2$ that contains bridging and chelating bpcd ligands has revealed a preference for electron accession at the chelating diphosphine ligand at the extended Hückel level [30]. Due to concern over the validity of the current calculations, vis-á-vis the site of electron accession, we also investigated cluster **4** at the extended Hückel level employing the X-ray fractional coordinates of **4**, as allowed by the CACAO program. Here two LUMO levels were found at −10.31 eV (bridging) and −10.22 eV (chelating) in excellent agreement with the data from the model cluster without phenyl groups. The factors that control the reduction selectively in these clusters that possess two distinct ligand acceptor sites are not clear and would benefit from additional examples before gross generalizations may be made with certainty.

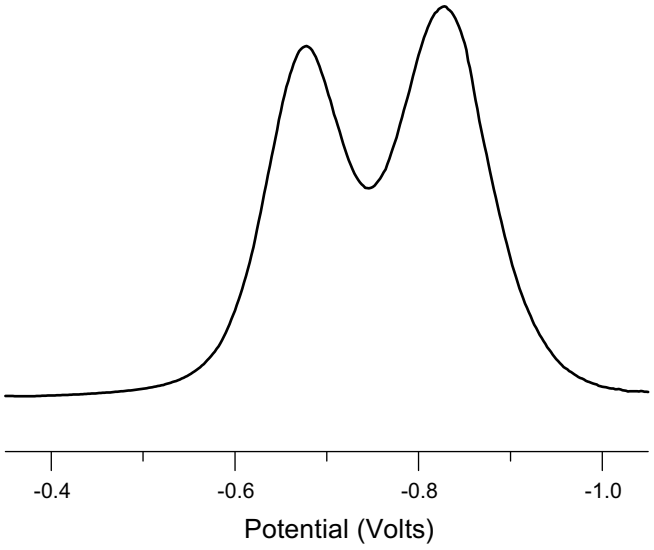

Fig. 3. Cathodic scan differential pulse voltammogram for cluster **4** in CH_2Cl_2 in 0.2 M TBAP at room temperature. The DPV was run at a scan rate of 20 mV/s and step time of 0.1 s.

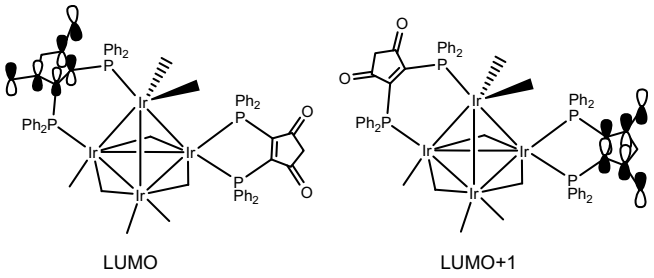

The redox properties of the hydride cluster **5** parallel those found in **4**. Two closely spaced one-electron reductions at $E_{1/2} = -0.65$ and −0.79 V were observed when a sample of **5** in CH_2Cl_2 containing 0.2 M TBAP was scanned over the potential range of 1.0 V to −1.2 V. Given the similarity of these redox data to those data found in cluster **4**, we assume that the two bpcd ligand ligands in **5** undergo sequential one-electron reductions in analogous fashion to cluster **4**. Here the bridging bpcd ligand in **5**,

which has also experienced an ortho metalation of one of its aryl groups, serves as the site-selective reservoir in the first electron accession.

4. Conclusions

Thermolysis of $Ir_4(CO)_{12}$ with the redox-active diphosphine ligand bpcd furnishes the mono- and disubstituted clusters $Ir_4(CO)_7(\mu\text{-}CO)_3$(bpcd) (**3**) and $Ir_4(CO)_5(\mu\text{-}CO)_3$(bpcd)(μ-bpcd) (**4**). The latter cluster is thermally unstable and readily loses CO to afford the hydride-bridged cluster $HIr_4(CO)_4(\mu\text{-}CO)_3$(bpcd)[μ-PhP($C_6H_4$)C=C($PPh_2$)-C(O)$CH_2$C(O)] (**5**). All three products have been characterized in solution and their solid-states structures determined by X-ray crystallography. The redox processes of clusters **3**–**5** have been explored, with the ancillary diphosphine ligand(s) serving as the site for the observed reduction chemistry. MO calculations corroborate the site-specific reduction behavior in the case of clusters **3** and **4**.

Acknowledgements

Financial support from the Robert A. Welch Foundation (Grants P-0074 to W.H.W. and B-1093 to M.G.R.) is appreciated.

Appendix A. Supplementary material

CCDC 606246, 606248 and 606247 contain the supplementary crystallographic data for the tetrairidium clusters **3**, **4** and **5**. These data can be obtained free of charge via http://www.ccdc.cam.ac.uk/conts/retrieving.html, or from the Cambridge Crystallographic Data Centre, 12 Union Road, Cambridge CB2 1EZ, UK; fax: (+44) 1223-336-033; or e-mail: deposit@ccdc.cam.ac.uk. Supplementary data associated with this article can be found, in the online version, at doi:10.1016/j.jorganchem.2007.07.016.

References

[1] (a) K.J. Karel, J.R. Norton, J. Am. Chem. Soc. 96 (1974) 6812;
(b) D.J. Darensbourg, M.J. Incorvia, J. Organomet. Chem. 171 (1979) 89;
(c) D.J. Darensbourg, M.J. Incorvia, Inorg. Chem. 19 (1980) 2585;
(d) D. Sonnenberger, J.D. Atwood, Inorg. Chem. 20 (1981) 3243;
(e) D.J. Darensbourg, B.J. Baldwin-Zuschke, Inorg. Chem. 20 (1981) 3846;
(f) D. Sonnenberger, J.D. Atwood, Organometallics 1 (1982) 694;
(g) D. Sonnenberger, J.D. Atwood, J. Am. Chem. Soc. 104 (1982) 2113;
(h) D.J. Darensbourg, B.J. Baldwin-Zuschke, J. Am. Chem. Soc. 104 (1982) 3906;
(i) K. Dahlinger, F. Falcone, A.J. Poë, Inorg. Chem. 25 (1986) 2654;
(j) J.R. Kennedy, P. Selz, A.L. Rheingold, W.C. Trogler, F. Basolo, J. Am. Chem. Soc. 111 (1989) 3615;
(k) N.M.J. Brodie, A.J. Poë, J. Organomet. Chem. 383 (1990) 531;
(l) B.F.G. Johnson, Y.V. Roberts, Inorg. Chim. Acta 205 (1993) 175;
(m) L. Chen, A.J. Poë, Coord. Chem. Rev. 143 (1995) 265;
(n) K.A. Bunten, D.H. Farrar, A.J. Poë, Organometallics 22 (2003) 3448.

[2] (a) For diphosphine derivatives from $Co_4(CO)_{12}$, see: N.J. Bailey, G. de Leeuw, J.S. Field, R.S. Haines, S. Afr. J. Chem. 38 (1985) 139;
(b) M.I. Bruce, A.J. Carty, B.G. Ellis, P.J. Low, B.W. Skelton, A.H. White, K.A. Udachin, N.N. Zaitseva, Aust. J. Chem. 54 (2001) 277;
(c) A. Choualeb, P. Braunstein, J. Rose, S.-E. Bouaoud, R. Welter, Organnometallics 22 (2003) 4405;
(d) H.A. Mirza, J.J. Vittal, R.J. Puddephatt, C.S. Frampton, L. Manojlovic-Muir, W. Xia, R.H. Hill, Organometallics 12 (1993) 2767;
(e) D.J. Darensbourg, D.J. Zalewski, A.L. Rheingold, R.L. Durney, Inorg. Chem. 25 (1986) 3281;
(f) S. Aime, R. Gobetto, G. Jannon, D. Osella, J. Organomet. Chem. 309 (1986) C51.

[3] (a) For diphosphine derivatives from $Rh_4(CO)_{12}$, see: K. Besancon, T. Lumini, G. Laurenczy, S. Detti, K. Schenk, R. Roulet, J. Chem. Soc., Dalton Trans. (2003) 968;
(b) F.H. Carre, F.A. Cotton, B.A. Frenz, Inorg. Chem. 15 (1976) 380;
(c) B. Moasser, W.L. Gladfelter, Inorg. Chim. Acta 242 (1996) 125;
(d) D.F. Foster, B.S. Nicholls, A.K. Smith, J. Organomet. Chem. 236 (1982) 395.

[4] (a) For diphosphine derivatives from $Ir_4(CO)_{12}$, see: M.M. Harding, B.S. Nicholls, A.K. Smith, Acta Crystallogr., Sect. C 40 (1984) 790;
(b) V.G. Albano, D. Braga, R. Ros, A. Scrivanti, J. Chem. Soc., Chem. Commun. (1985) 866;
(c) R. Ros, A. Scrivanti, V.G. Albano, D. Braga, L. Garlaschelli, J. Chem. Soc., Dalton Trans. (1986) 2411;
(d) A. Strawczynski, R. Ros, R. Roulet, D. Braga, C. Gradella, F. Grepioni, Inorg. Chim. Acta 170 (1990) 17;
(e) G. Laurenczy, G. Bondietti, R. Ros, R. Roulet, Inorg. Chim. Acta 247 (1996) 65;
(f) D. Tranqui, A. Durif, M.N. Eddine, J.L. Lieto, J.J. Rafalko, B.C. Gates, Acta Crystallogr., Sect. B 38 (1982) 1916;
(g) T. Lumini, G. Laurenczy, R. Roulet, A. Tassan, R. Ros, K. Schenk, G. Gervasio, Helv. Chim. Acta 81 (1998) 781;
(h) N. Nawar, J. Organomet. Chem. 602 (2000) 137;
(i) B.K. Park, M.A. Miah, H. Kang, K. Lee, Y.-J. Cho, D.G. Churchill, S. Park, M.-G. Choi, J.T. Park, Organometallics 24 (2005) 675.

[5] R.D. Pergola, L. Garlaschelli, S. Martinengo, J. Organomet. Chem. 331 (1987) 271.

[6] P. Chini, G. Ciani, L. Garlaschelli, M. Manassero, S. Martinengo, A. Sironi, F. Canziani, J. Organomet. Chem. 152 (1978) C35.

[7] (a) D. Fenske, H. Becher, Chem. Ber. 107 (1974) 117;
(b) D. Fenske, Chem. Ber. 112 (1979) 363.

[8] D.F. Shriver, The Manipulation of Air-Sensitive Compounds, McGraw-Hill, New York, 1969.

[9] SAINT Version 6.02, Bruker Analytical X-ray Systems, Inc. Copyright 1997–1999.

[10] SHELXTL Version 5.1, Bruker Analytical X-ray Systems, Inc. Copyright 1998.

[11] A.L. Spek, PLATON – A Multipurpose Crystallographic Tool, Utrecht University, Utrecht, The Netherlands, 2001.

[12] A.J. Bard, L.R. Faulkner, Electrochemical Methods, Wiley, New York, 1980.

[13] (a) R. Hoffmann, W.N. Lipscomb, J. Chem. Phys. 36 (1962) 2179;
(b) R. Hoffmann, J. Chem. Phys. 39 (1963) 1397.

[14] C. Mealli, D.M. Proserpio, J. Chem. Educ. 67 (1990) 399.

[15] R.C. Weast (Ed.), Handbook of Chemistry and Physics, 56th ed., CRC Press, Cleveland, OH, 1975.

[16] (a) P. Chini, G. Ciani, L. Garlaschelli, M. Manassero, S. Martinengo, A. Sironi, F. Canziani, J. Organomet. Chem. 152 (1978) C35;
(b) A. Orlandi, R. Ros, R. Roulet, Helv. Chim. Acta 74 (1991) 1464;
(c) K. Besancon, G. Laurenczy, T. Lumini, R. Roulet, G. Gervasio, Helv. Chim. Acta 76 (1993) 1993.

[17] Control experiments confirm that cluster **3** and bpcd when treated with Me_3NO or direct thermolysis of cluster **3** with bpcd afford cluster **4** in good yields.

[18] N.B. Coltrup, L.H. Daly, S.E. Wiberley, Introduction to Infrared and Raman Spectroscopy, Academic Press, New York, 1990.
[19] (a) L. Garlaschelli, S. Martinengo, P. Chini, F. Canziani, R. Bau, J. Organomet. Chem. 213 (1981) 379;
(b) M.R. Churchill, J.P. Hutchinson, Inorg. Chem. 20 (1981) 4112;
(c) R. Bau, M.Y. Chiang, C.-Y. Wei, L. Garlaschelli, S. Martinengo, T.F. Koetzle, Inorg. Chem. 23 (1984) 4758;
(d) D.J. Darensbourg, F.A. Beckford, J.H. Reibenspies, J. Cluster Sci. 11 (2000) 95;
(e) A.M. Arif, D.E. Heaton, R.A. Jones, K.B. Kidd, T.C. Wright, B.R. Whittlesey, J.L. Atwood, W.E. Hunter, H. Zhang, Inorg. Chem. 26 (1987) 4065.
[20] J.R. Shapley, G.F. Stuntz, M.R. Churchill, J.P. Hutchinson, J. Am. Chem. Soc. 101 (1979) 7425.
[21] (a) H. Shen, S.G. Bott, M.G. Richmond, Organometallics 14 (1995) 4625;
(b) S.G. Bott, J.C. Wang, H. Shen, M.G. Richmond, J. Chem. Crystallogr. 29 (1999);
(c) C.-G. Xia, S.G. Bott, G. Wu, M.G. Richmond, J. Chem. Crystallogr. 34 (2004) 513;
(d) W.H. Watson, S. Kandala, M.G. Richmond, J. Chem. Crystallogr. 35 (2005) 157.
[22] (a) K. Yang, J.M. Smith, S.G. Bott, M.G. Richmond, Organometallics 12 (1993) 4779;
(b) S.G. Bott, H. Shen, M.G. Richmond, Struct. Chem. 12 (2001) 225.
[23] For related examples demonstrating this phenomenon, see: W.H. Watson, G. Wu, M.G. Richmond, Organometallics 24 (2005) 5431; W.H. Watson, G. Wu, M.G. Richmond, Organometallics 25 (2006) 930.
[24] M.G. Richmond, J.K. Kochi, Inorg. Chem. 25 (1986) 1334.
[25] D.M.P. Mingos, D.J. Wales, Introduction to Cluster Chemistry, Prentice-Hall, Englewood Cliffs, NJ, 1990.
[26] (a) H. Jungbluth, G. Süss-Fink, M.A. Pellinghelli, A. Tiripicchio, Organometallics 9 (1990) 1670;
(b) S.M. Waterman, V.-A. Tolhurst, M.G. Humphrey, B.W. Skelton, A.H. White, J. Organomet. Chem. 515 (1996) 89;
(c) C.-H. Ueng, S.-M. Lu, Inorg. Chim. Acta 262 (1997) 113;
(d) M.H. de Araujo, M.D. Vargas, D. Braga, F. Grepioni, Polyhedron 17 (1998) 2865;
(e) R.D. Adams, B. Captain, J.L. Smith Jr., Inorg. Chem. 44 (2005) 1413.
[27] (a) Here the diffusion-controlled reduction was deemed reversible based on the data obtained from plots of the current function I_p^a versus the square root of the scan rate, unity current ratios, and the magnitude of the peak-to-peak separation (ΔE_p) of the cathodic (E_p^c) and anodic (E_p^a) waves;
(b) For the criteria that define an electrochemical reversible redox process, see: P.H. Rieger, Electrochemistry, Chapman & Hall, New York, 1994.
[28] (a) K. Hayakawa, N. Mibu, E. Osawa, K. Kanematsu, J. Am. Chem. Soc. 104 (1982) 7136;
(b) T.A. Albright, J.K. Burdett, M.H. Whangbo, Orbital Interactions in Chemistry, Wiley, New York, 1985.
[29] (a) We have also performed extended Hückel MO calculations on the model compound 1,1-$Ir_4(CO)_7(\mu\text{-}CO)_3(PH_3)_2$ to probe the nature of the LUMO in a cluster containing redox inactive phosphine ligands. Our calculations revealed a LUMO at −9.58 eV, whose orbital composition consisted of antibonding Ir–Ir interactions, in keeping with the reported redox chemistry and MO properties of simple polynuclear iridium clusters: B.M. Peake, B.H. Robinson, J. Simpson, D. Watson, J. Chem. Soc., Chem. Commun. (1974) 945;
(b) L. Malatesta, G. Caglio, M. Angoletta, J. Chem. Soc., Chem. Commun. (1970) 532;
(c) D. Braga, F. Grepioni, J.J. Byrne, M.J. Calhorda, J. Chem. Soc., Dalton Trans. (1995) 3287.
[30] S.G. Bott, H. Shen, M.G. Richmond, J. Organomet. Chem. 689 (2004) 3426.